Identification of Elasto-Plastic Property of Aluminium Alloy Under Multiple Mechanical Tests

M. Uchida[1a] and M. Nakayama[1]

[1]Gakuen-cho, Nakaku, Sakai, Osaka, 599-8531, JAPAN

[a]m_uchida@omu.ac.jp

Abstract. In the conventional material identification process, the stress–strain curve is obtained through mechanical tests such as tensile testing and is modeled using a constitutive equation. In contrast, recent identification methods have shifted toward evaluating both the mechanical response and the strain field by integrating digital image correlation (DIC) with the finite element method (FEM). However, this approach requires a considerable computational cost because the FEM boundary-value problem must be repeatedly solved for tentative material parameters during the iterative identification process. In this study, the FEM boundary-value problem is replaced by an approximation function derived from a machine-learning (ML) model trained on preliminarily computed FEM results with varied material parameters. Using the proposed ML-assisted material identification procedure based on the DIC–FEM coupling scheme, the elastic–plastic properties of an aluminum alloy are evaluated.

Constitutive Model

The following typical multiaxial constitutive equation for the elasto-plastic material is employed in the FEM simulation.

$$\dot{\hat{\boldsymbol{S}}} = \left(\boldsymbol{D}^e - \frac{9G}{(3G+h)}\cdot\frac{\boldsymbol{\sigma}'\otimes\boldsymbol{\sigma}'}{\bar{\sigma}^2}\right):\dot{\boldsymbol{\varepsilon}} \tag{1}$$

were $\dot{\hat{\boldsymbol{S}}}$ is the Jauman rate of Kirchhoff stress, $\boldsymbol{D}^e$ is the elastic modulus tensor, G is shear modulus, h is hardening rate, $\boldsymbol{\sigma}'$ is the deviatoric stress, $\bar{\sigma}$ is the equivalent stress, and $\dot{\boldsymbol{\varepsilon}}$ is the strain rate. Hardening rate is obtained by determining the stress-strain curve obtained from the experiment. The object material employed in this study is aluminium alloy, which shows a yield plateau in the earlier stage of the deformation. The following phenomenological constitutive equation, which is the sum of the conventional power law and the additional yield plateau stress terms, was employed to represent the mechanical response of the material:

$$\bar{\sigma} = K\bar{\varepsilon}^n + \frac{A}{1+\exp\{a(\bar{\varepsilon}-\varepsilon_0)\}} \tag{2}$$

where K, n, A, a, and ε_0 are material constants. In the identification process, these parameters were determined so that the following error function is minimized:

$$\Phi = \alpha\sum_{I=1}^{N_\varepsilon}\{\varepsilon_I^{DIC} - \varepsilon(\boldsymbol{\theta})_I^{FEM}\}^2 + \beta\sum_{J=1}^{N_L}\{f_J^{LC} - f(\boldsymbol{\theta})_J^{FEM}\}^2 \tag{3}$$

where ε_I^{DIC} and f_J^{LC} are local strain measured by DIC and load obtained from the load cell, $\varepsilon(\boldsymbol{\theta})_I^{FEM}$ and $f(\boldsymbol{\theta})_J^{FEM}$ are local strain and load predicted by FEM with material parameter set $\theta = (E,\nu,K,n,A,a,\varepsilon_0)^T$, E is Young's modulus, ν is Poisson's ratio, α and β are weight parameters. The material parameter set minimizing the error function can be explored by solving the following differential equation:

$$\frac{\partial\Phi}{\partial\boldsymbol{\theta}} = \alpha\sum_{I=1}^{N_\varepsilon}\{\varepsilon_I^{DIC} - \varepsilon(\boldsymbol{\theta})_I^{FEM}\}\frac{\partial\varepsilon(\boldsymbol{\theta})_I^{FEM}}{\partial\boldsymbol{\theta}} + \beta\sum_{J=1}^{N_L}\{f_J^{LC} - f(\boldsymbol{\theta})_J^{FEM}\}\frac{\partial f(\boldsymbol{\theta})_I^{FEM}}{\partial\boldsymbol{\theta}} = 0 \tag{4}$$

To solve this nonlinear simultaneous Eq. (4), we employ the Newton-Raphson iterative scheme. In this process, the material parameter set is updated by iterative calculation using the following equation:

$$\begin{aligned}\boldsymbol{\theta}^{k+1} = \boldsymbol{\theta}^k &+ \alpha\sum_{I=1}^{N_\varepsilon}\left\{\frac{\partial\varepsilon(\boldsymbol{\theta})_I^{FEM}}{\partial\boldsymbol{\theta}}\otimes\frac{\partial\varepsilon(\boldsymbol{\theta})_I^{FEM}}{\partial\boldsymbol{\theta}}\right\}^{-1}:\{\varepsilon_I^{DIC} - \varepsilon(\boldsymbol{\theta})_I^{FEM}\}\frac{\partial\varepsilon(\boldsymbol{\theta})_I^{FEM}}{\partial\boldsymbol{\theta}} \\ &+\beta\sum_{J=1}^{N_L}\left\{\frac{\partial f(\boldsymbol{\theta})_I^{FEM}}{\partial\boldsymbol{\theta}}\otimes\frac{\partial f(\boldsymbol{\theta})_I^{FEM}}{\partial\boldsymbol{\theta}}\right\}^{-1}:\{f_J^{LC} - f(\boldsymbol{\theta})_J^{FEM}\}\frac{\partial f(\boldsymbol{\theta})_I^{FEM}}{\partial\boldsymbol{\theta}} = 0\end{aligned} \tag{5}$$

where k is the iteration counter.

In the iterative calculation, the FEM boundary-value problem must be solved to obtain the derivatives of the error function with respect to all parameters. This results in a substantial computational burden during the identification process. In this study, a machine-learning (ML) scheme is introduced to approximate the FEM results without directly solving the boundary-value problem. The input data for the ML model consist of the uniaxial mechanical response corresponding to a given tentative parameter set, which can be computed immediately by solving the multiaxial constitutive equation under uniaxial loading conditions. The output data are the approximated FEM results required to evaluate the error function in Eq. (3). The approximation function is constructed using the ML scheme trained on preliminary FEM simulations. For this purpose, FEM analyses with various parameter sets were performed in advance, and the resulting data were used as training samples to build the approximation function.

Validation

To evaluate the identification accuracy of the proposed method, a virtual experiment was conducted using FEM simulations with known material parameters. In the proposed approach, the approximated FEM results are obtained immediately through the ML-based approximation function, eliminating the need to solve the boundary-value problem directly. This enables relatively high-speed identification even when multiple mechanical tests are incorporated into the process. Material parameters identified using multiple mechanical tests are more generalizable, as they can be applied to various mechanical conditions, including multiaxial and non-uniform stress states. Figure 1 shows the FEM models used in the virtual experiment. The square and notched models were prepared to assess the accuracy of the proposed method.

Table 1 summarizes the given and identified material parameters, along with their relative errors. Young's modulus E and the parameters K and A, which have units of Pa, were identified with reasonable accuracy. In contrast, Poisson's ratio ν and the parameters a and ε_0, which are dimensionless, exhibited relatively larger errors. The former parameters primarily characterize the stress–strain response, whereas the latter parameters mainly describe non-uniform deformation and the yield plateau. The mechanical conditions used in the verification test were insufficient to accurately identify these latter parameters. Figure 2 shows the evolution of the strain fields obtained from FEM simulations of the notched model using both the given and identified parameters. Because the strain fields are nearly identical, the sensitivity of the strain distribution to variations in these material parameters is low. Additional mechanical tests would improve the identification accuracy.

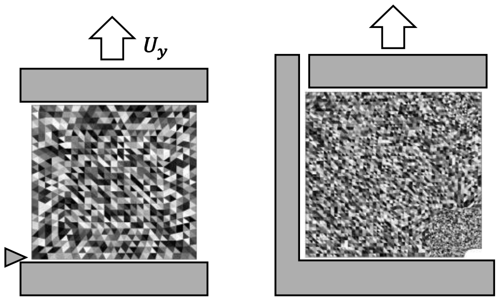

(a) Square model (b) Notched model

Fig. 1 FEM model for virtual experiment

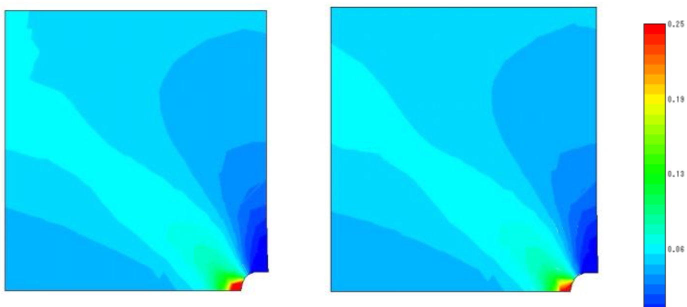

(a) Given parameters (b) Identified parameters

Fig. 2 Strain fields obtained from FEM calculations with given and identified parameters.

Table 1 Given and identified material parameters

	E [MPa]	ν	K [MPa]	n	A [MPa]	a	ε_0
Given parameter	62400	0.33	423	0.25	54.2	410	0.0042
Identified result	60108	0.29	430	0.26	53.2	432	0.0032
Relative error, %	3.67	12.0	1.65	4.0	1.85	5.37	24.0

Conclusion

To enhance the efficiency of material identification based on the DIC–FEM coupling method, a machine-learning (ML) approach was introduced to approximate FEM simulation results. This enables the incorporation of multiple mechanical conditions into the parameter identification process. Although the identification accuracy obtained in the virtual experiment was not fully satisfactory, it is expected to improve with the inclusion of additional mechanical tests that exhibit higher sensitivity to the material parameters.